IEEE Photonics Journal
An IEEE Photonics Society Publication

Open Access

Low-Power Operation in a Silicon Switch Based on an Asymmetric Mach–Zehnder Interferometer

Volume 7, Number 2, April 2015

L. Sanchez
A. Griol
S. Lechago
A. Brimont
P. Sanchis

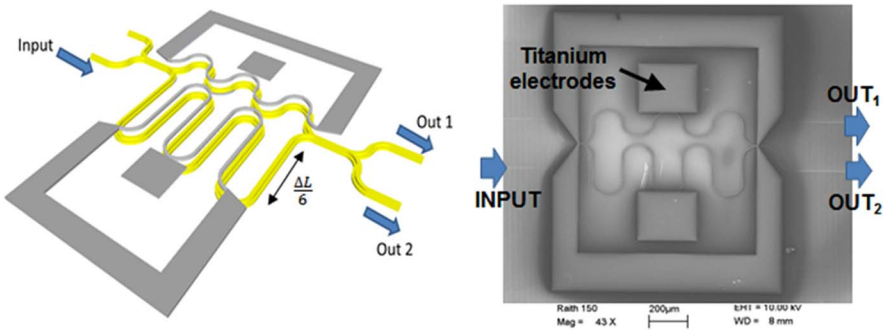

DOI: 10.1109/JPHOT.2015.2407317
1943-0655 © 2015 IEEE

IEEE photonics SOCIETY

IEEE

Low-Power Operation in a Silicon Switch Based on an Asymmetric Mach–Zehnder Interferometer

L. Sanchez, A. Griol, S. Lechago, A. Brimont, and P. Sanchis

Nanophotonics Technology Center, Universitat Politecnica de Valencia, 46022 Valencia, Spain

DOI: 10.1109/JPHOT.2015.2407317

Manuscript received February 4, 2015; revised February 23, 2015; accepted February 23, 2015. Date of publication February 28, 2015; date of current version March 10, 2015. This work was supported by TEC2012-38540 LEOMIS and NANOMET PLUS-Conselleria d'Educacio, Cultura i Esport-PROMETEOII/2014/034. The work of L. Sanchez was supported by Generalitat Valenciana in the context of the VALi+d program. Corresponding author: P. Sanchis (e-mail: pabsanki@ntc.upv.es).

Abstract: Mach–Zehnder interferometer (MZI) structures are widely used as optical switches in photonic integrated circuits. However, power consumption is still the key parameter to make such devices practical in the silicon platform, particularly for those based on the thermo-optic effect. A new approach to significantly decrease the power consumption of a silicon switch based on an asymmetric MZI, together with an optimum selection of the operation wavelengths, is proposed. A power consumption reduction up to 50% is experimentally demonstrated in agreement with simulation results.

Index Terms: Integrated optics, optical switches and silicon photonics.

1. Introduction

Silicon technology based on the silicon on insulator platform (SOI) have experienced an enormous development during the last decades, and silicon photonic building blocks like modulators, filters, detectors, or switches have been improved in terms of speed, sensitivity, power consumption and losses [1]. Ring resonators and Mach–Zehnder interferometric structures (MZIs) are the most common structures for optical switches in photonic integrated circuits. MZI-based switches exhibit broadband spectral operation and their electro-optic switching performance may be achieved using the thermo-optic (TO) or the plasma dispersion effects. The TO effect suffers from higher power consumption and is slower than the plasma dispersion effect, but it enables larger phase shifts per unit length due to silicon's high thermo-optic coefficient, and it is also fast enough for switching applications.

In order to achieve a better performance than current electrical networks, optical networks will require low power consumption, low latency and high bandwidth [2]–[4]. To achieve this, it is necessary to improve optical switching matrices which overall performance is directly related to the characteristics of their optical switches. Therefore, a key point to improve is the efficiency and power consumption of optical switches (based on ring resonators [5]–[7] or MZI structures [9]–[17]) in order to obtain high performance optical networks. MZI-based optical switches using the TO effect feature high efficiency but usually require their power consumption to be reduced in order to ensure low power operation. Recent works showing a 4×4 switch with a power consumption below 20.4 mW for a bandwidth per port of 40 Gbps [9], a

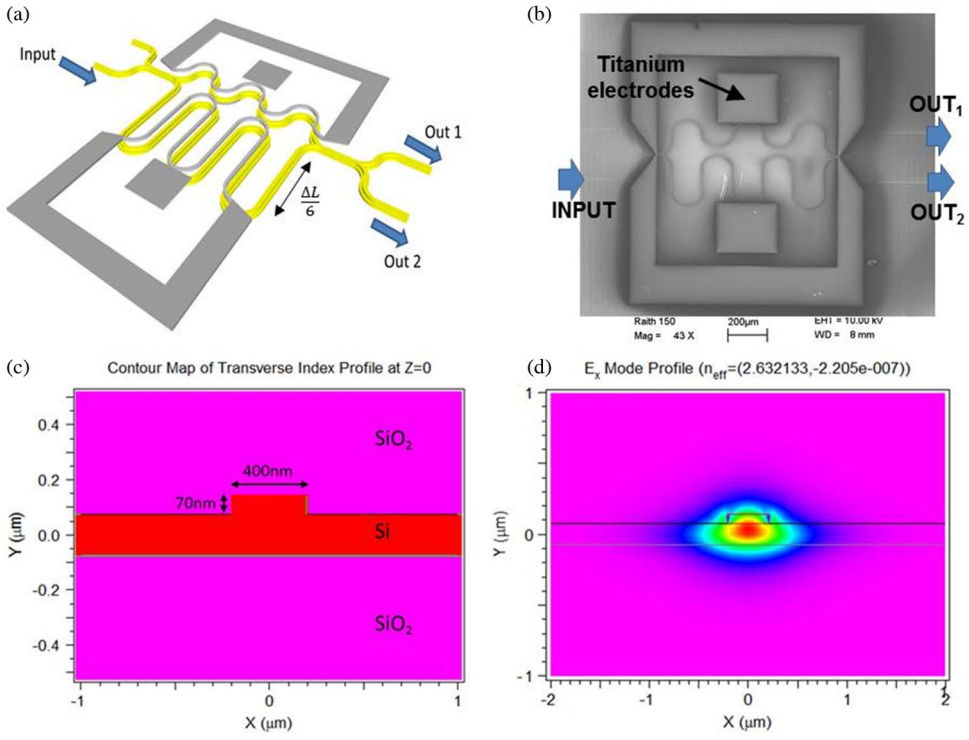

Fig. 1. (a) 3-D schematic of the a-MZI switching structure, where ΔL is the length difference between the MZI arms, (b) SEM image of fabricated device, (c) cross section of the rib waveguide and refractive index distribution, and (d) fundamental transverse electric (TE) mode of the rib waveguide.

2 × 2 non-blocking switch matrix based on MZI with a total power consumption which varies from 4.55 mW to 22.4 mW, depending on the switching state and physical path [11], a Mach-Zehnder-based five-port silicon router with a consumed power of 25 mW [13], or a Mach-Zehnder-based four port switching module with a power consumption from 9 mW to 42.6 mW [10] have been demonstrated.

In this paper, we propose a novel approach to minimize the power consumption required for switching between two states. The approach is based on taking advantage of the periodic response of the transmission spectrum in an asymmetric MZI (a-MZI) structure. Switching power consumption reduction from 32% to 50% is experimentally demonstrated for bit rates ranging from 10 to 30 Gbps introducing only an extra level of insertion losses below 0.5 dB.

2. Device Design

Fig. 1(a)–(d) show respectively the 3-D schematic of the a-MZI switching structure, a scanning electron microscope (SEM) image of the fabricated device, the cross section of the considered waveguide and the fundamental transverse electric mode. The a-MZI is based on a shallow-etched rib waveguide with 70 nm-deep sidewalls. Multimode interferometers have been used at the input and the output of the MZI to split and recombine the signals. The electrodes have a configuration with central fed to achieve a better distribution of the heat from the center to the sides, thus obtaining a more gradual change in the refractive index.

Fig. 2 shows the simulated optical power at both output ports as a function of the wavelength for (a) the symmetric MZI (s-MZI) structure and (b) the a-MZI structure without applying any electrical power. The switching performance in the a-MZI can be understood by looking at the evolution of the transmission spectrum as a function of the applied electrical power. Therefore, Fig. 2 shows also the output optical power as a function of the wavelength for (d) the s-MZI and

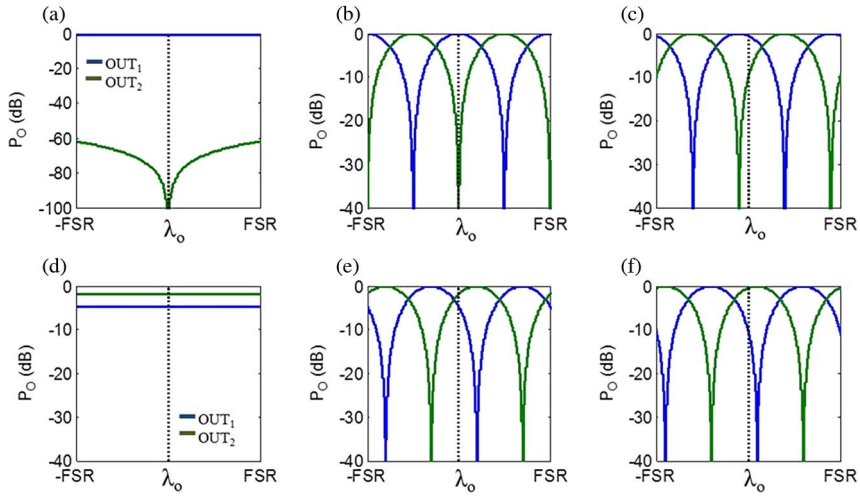

Fig. 2. Simulated output optical power as a function of the wavelength for the s-MZI structure and the a-MZI structure with $\gamma = 0$ and $\gamma = 0.2$, taking into account a normalized applied electrical power of (a)–(c) $P/P_\pi = 0$ and (d)–(f) $P/P_\pi = 0.6$, respectively.

(e) the a-MZI structures when a normalized electrical power P/P_π of 0.6 is applied. P_π is the power required for achieving a phase shift of π radians.

It can be seen that the periodic response in the a-MZI structure maintains the same shape but is wavelength shifted. Therefore, by choosing an operation wavelength shifted with respect to the central wavelength, two identical switching states can be achieved with much less electrical power than in the s-MZI, as it is shown in Fig. 2(c) and (f). The operation wavelength, λ_o, can be defined as

$$\lambda_o = \lambda_{\max} + \gamma \cdot \frac{\mathrm{FSR}}{2} \tag{1}$$

where $\lambda_{\max}$ is the wavelength at which the maximum output power is achieved in one of ports without applying any electrical power, FSR is the free spectral range of the a-MZI, and γ is a design parameter directly related with the reduction in power consumption. The output optical power as a function of the wavelength for the a-MZI structure with $\gamma = 0.2$ is shown in Fig. 2(c) without applying electrical power and Fig. 2(f) applying an electrical power of $0.6P_\pi$. If $\gamma = 0.2$, only $0.6P_\pi$ is required to switch from the cross state, shown in Fig. 2(c), to the bar state, shown in Fig. 2(f). On the other hand, P_π is always required in the s-MZI, as well in the a-MZI with $\gamma = 0$, to complete the switching because otherwise high insertion losses and unacceptable crosstalk would be given in the bar state, as it can be seen in Fig. 2(d) and (e), respectively.

The percentage of power consumption reduction in the a-MZI is around two times the γ-parameter (for example the required electrical power has been reduced in a 40% when the γ-parameter is 0.2). However, it can also be seen in both Fig. 2(c) and (e) that there is a penalty on insertion losses and crosstalk. Such penalty as a function of the γ-parameter is depicted in Fig. 3. It can be seen that the influence on the insertion losses is almost negligible while a low crosstalk can also be achieved. Using a γ-parameter below 0.25, insertion losses below 1 dB and crosstalk values above 10 dB will be achieved.

It is important to notice that the change in the operation wavelength only implies that the optical response of the a-MZI switch would be designed to fit with the wavelengths used in the system. Therefore, once λ_o is defined, $\lambda_{\max}$ would be obtained from (1) and used to calculate

$$N = \frac{2n_{\mathrm{eff}}\lambda_{\max}}{n_g \mathrm{FSR}} \tag{2}$$

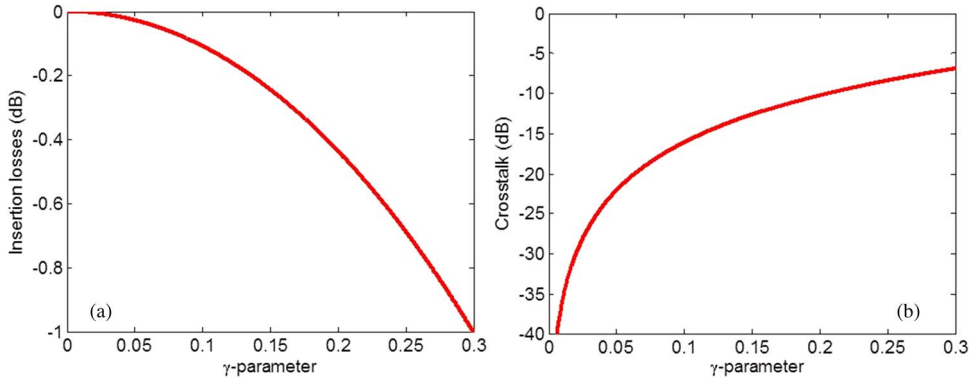

Fig. 3. Penalty on (a) insertion losses and (b) crosstalk as a function of γ-parameter in the proposed a-MZI switching structure.

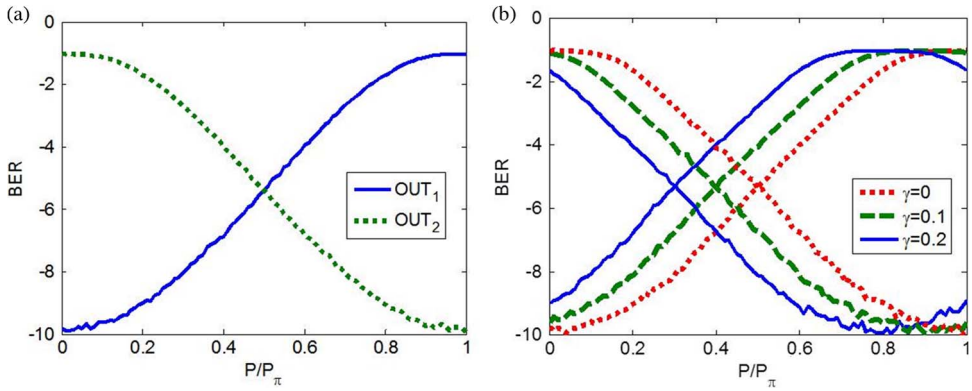

Fig. 4. Simulated BER as a function of the normalized applied electrical power for (a) the s-MZI and for (b) the a-MZI for different γ-parameter values.

where n_{eff} and n_g is the effective and group indices of the optical waveguide. In such a way, the required length difference, shown in Fig. 1(a), will be obtained as

$$\Delta L = \frac{N_{\text{even}} \lambda_{\max}}{2 n_{\text{eff}}} \tag{3}$$

where N_{even} is the closest even integer to N. In our case, the group index is 3.619 and $\lambda_{\max}$ and the free spectral range have been set to 1550 nm and 100 GHz, respectively. Hence, the required length difference between the arms of the a-MZI is 830 μm.

System simulations have also been carried out to analyze the influence of the a-MZI spectral response on the switching performance. Simulations have been done in Matlab© and considering white Gaussian noise and a non-return-to-zero (NRZ) digital signal. The bit error rate (BER) in the s-MZI as a function of the applied electrical power (normalized by P_π) is shown at both output ports in Fig. 4(a). The FSR is 100 GHz, the bit rate of the digital signal is 10 Gbps, and the signal-to-noise ratio (SNR) is 13 dB. The response of the outputs is complementary and there are two different states. Without applying any power, the cross state, output one (OUT_1) is in error free level (lower than 10^{-9}), while output two (OUT_2) has a very high BER level. It means that almost all the input signal is switched to OUT_1 port and only a negligible portion is undesirably switched to OUT_2 port due to the crosstalk. By applying P_π, the bar state, the switching is reversed and the input signal is now switched to OUT_2 port so that the output signal is in error free.

Fig. 4(b) shows the BER as a function of the normalized applied electrical power in the a-MZI switch at both output ports and for different values of the γ-parameter. The red dotted line is for

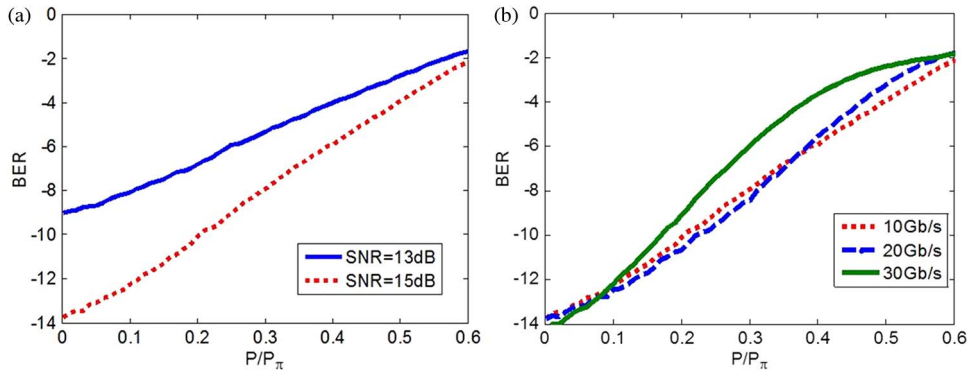

Fig. 5. Simulated BER as a function of the normalized applied electrical power for the a-MZI with $\gamma = 0.2$ and different values of (a) signal-to-noise ratio and (b) data bit rate.

$\gamma = 0$. Therefore, the a-MZI is working at the central wavelength and the switching response is almost identical to that of the s-MZI depicted in Fig. 4(a). Therefore, the required power to complete the switching in the a-MZI is also P_π. However, when the γ-parameter is increased to 0.1 (green dotted line), the switching from the error free level to a high error level is accomplished with around a 20 percent less power consumption. It is important to notice that the same error levels at both output ports are required at the two switching states, i.e., $P/P_\pi = 0$ and $P/P_\pi = 0.8$ for $\gamma = 0.1$, to have the same conditions of insertion losses and crosstalk. On the other hand, for an applied electrical power equal to zero, the BER is a bit higher than for $\gamma = 0$ but it is still in error free confirming that the impact on insertion losses is almost negligible. For $\gamma = 0.2$ (blue line), a significant power reduction of around 40% is achieved as only $P/P_\pi = 0.6$ is required for switching between the two states.

The influence of other parameters like the SNR or the bit rate has also been also analyzed. Fig. 5(a) shows that, for a fixed value of $\gamma = 0.2$ and a bit rate of 10 Gbps, increasing the SNR from 13 to 15 improves the BER level at the cross state, i.e., $P/P_\pi = 0$, but it is important to notice that this does not mean a reduction in power consumption because a high error level must be achieved for complete switching to the bar state. Therefore, $0.6P_\pi$ is always required for $\gamma = 0.2$ to switch between the bar and cross states independently of the SNR value. On the other hand, Fig. 5(b) shows the influence of the bandwidth of the signal for a fixed FSR of 100 GHz, a SNR of 15 and $\gamma = 0.2$. When the bit rate is increased, higher values of BER may be achieved with a lower applied electrical power due to the filtering effect of the spectral response of the a-MZI structure, but in the end, the amount of power to complete the switching is again the same independently of the bit rate. Therefore, adjusting the FSR as a function of the bit rate does not provide a reduction in power consumption but it is interesting for introducing several channels simultaneously. It should be noticed that by inserting several channels in the pass bands of the a-MZI a wide optical bandwidth can be achieved as it has also been proposed for ring based switches [19].

3. Experimental Results

The a-MZI switch has been fabricated to experimentally demonstrate the proposed approach to reduce the power consumption. In order to avoid any influence of the electrodes, the same structure has been measured and compared at the central wavelength, in which the performance is like in a s-MZI, and working with different operation wavelengths. The device was fabricated on standard SOI samples of SOITEC wafers with a top silicon layer thickness of 220 nm and a buried oxide layer thickness of 2 μm. The structure fabrication is based on an electron beam direct writing process performed on a coated 100 nm hydrogen silsesquioxane (HSQ) resist film. After developing the HSQ resist using TMAH as developer, the resist patterns were transferred into the SOI samples employing an also optimized Inductively Coupled

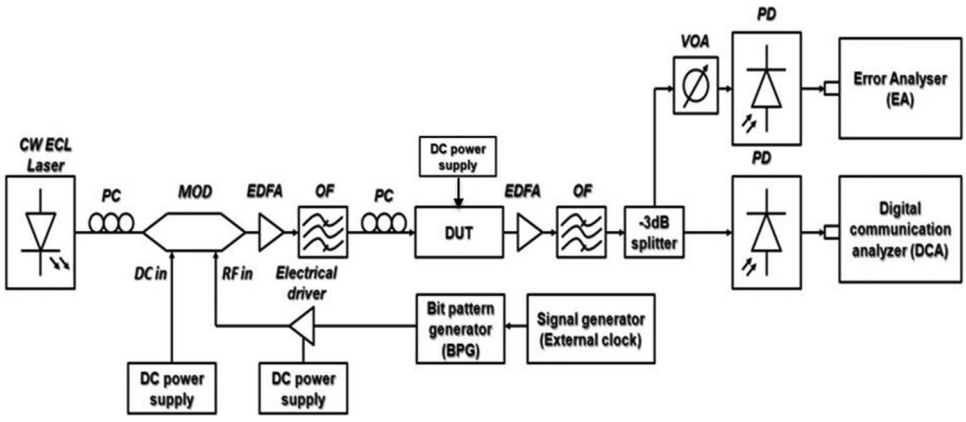

Fig. 6. Experimental set-up.

Plasma-Reactive Ion Etching process with fluoride gases (SF6/C4F8). The etching process was optimized to reach 70 nm deep structures (rib waveguides). Once the silicon is etched, the samples were covered with 0.7 microns of silicon dioxide deposited by means of PECVD tool. Finally, Titanium microheaters were placed on the tuning structures by evaporation and a lift-off process.

Fig. 6 illustrates the experimental set-up. A commercial $LiNbO_3$ modulator fed with a 10–30 Gbps NRZ pseudo-random bit sequence (PRBS $2^{31}-1$) delivered by a bit pattern generator is used. The electrical signal was amplified through a broad bandwidth driver amplifier (DC to 40 GHz) to achieve a voltage swing of $\sim$5 Vpp and combined to a 1.7 V DC offset to ensure the modulator is biased at quadrature. The input modulated signal was amplified and filtered with an optical filter of 3 nm to decrease the noise introduced by the EDFA. Then, the signal was coupled in and out the silicon chip via grating couplers. An EDFA after the device amplifies its output signal and a 3 dB splitter divides the power for simultaneously measuring the eye diagram and the BER. The signal was then photodetected by a 40 GHz Digital Communication Analyzer to see the eye diagram and the BER was measured by means of a 75 GHz photodiode connected to the Error Analyzer and evaluated as a function of the electrical power applied to the device under test (DUT).

Several measurements of the BER value as function of the applied electrical power to the electrodes have been carried out. First, the a-MZI switch has been characterized at the central wavelength of the spectral response, as it was depicted in Fig. 2(b). BER measurements as a function of the applied power normalized by P_π are shown in Fig. 7(a) for bit rates between 10 to 30 Gbps and $\gamma = 0$. Without applying electrical power, error free performance was achieved for all the bit rates under study. If the bit rate of the signal increases, higher BER values are achieved for electrical powers above $0.5P_\pi$, in agreement with simulations results depicted in Fig. 5(b). However, it is important to remind that this does not mean that power consumption is lower because to complete the switching an electrical power of P_π is required.

The switching performance has been compared with the device working at different operation wavelengths. Results are shown in Fig. 7(b)–(d). It can be clearly seen that, for a certain bit rate, the same value of BER is achieved with an important reduction in the applied electrical power. For example, in Fig. 7(b), to obtain a variation from error free to 10^{-4} BER level by using $\gamma = 0.24$ and a bit rate of 10 Gbps, the power reduction comparing with the same structure working at the central wavelength $(\gamma = 0)$ is around 50% in agreement with simulation results. Fig. 7(c) and (d) show that the power reduction is lower, independently of the used bit rate, when the γ-parameter is decreased. A power reduction of around 40% is demonstrated for $\gamma = 0.2$ and around 32% for $\gamma = 0.16$, which is once more in agreement with simulation results. In our device, a P_π power of 36 mW was measured. Therefore, the proposed approach would allow reducing the power consumption up to 18 mW with respect to a conventional s-MZI switch.

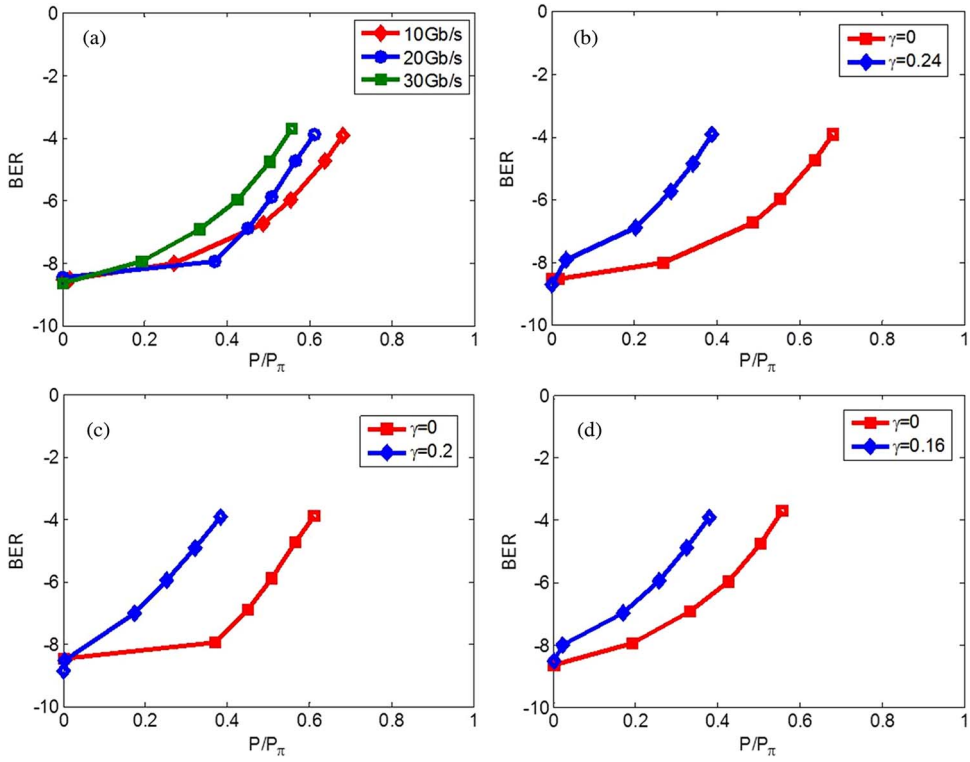

Fig. 7. BER as function of the normalized applied power for (a) $\gamma = 0$ and different bit rates, (b) 10 Gbps, (b) 20 Gbps, and (c) 30 Gbps.

4. Conclusion

A novel approach has been proposed and analyzed by means of simulations and experimentally demonstrated to decrease the power consumption in silicon switches. The switch is based on an asymmetric MZI structure and operated with a conveniently chosen wavelength. The latter only implies that the optical response of the a-MZI switch would be designed to fit with the wavelengths used in the system. A power consumption reduction up to 50% has been demonstrated which could open a new path for energy efficient switching in silicon via the thermo-optic effect.

References

[1] B. Jalali and S. Fathpour, "Silicon photonics," *IEEE J. Lightw. Technol.*, vol. 24, no. 12, pp. 4600–4615, Dec. 2006.
[2] M. A. Taubenblatt, J. A. Kash, and Y. Taira, "Optical interconnects for high performance computing," in *Proc. Commun. Photon. Conf. Exhib.*, 2009, pp. 1–2.
[3] D. Kalavrouziotis *et al.*, "Active plasmonics in true data traffic applications: Thermo-optic ON/OFF gating using a silicon-plasmonic asymmetric Mach–Zehnder interferometer," *IEEE Photon. Technol. Lett.*, vol. 24, no. 12, pp. 1036–1038, Jun. 2012.
[4] K. Bergman, "Photonic networks for intra-chip, inter-chip, and box-to-box interconnects in high performance computing," in *Proc. Opt. Commun. ECOC Eur. Conf.*, 2006, pp. 1–64.
[5] B. C. Lin and C. T. Lea, "Exploiting two-wavelength switching capability of silicon photonic microrings," *IEEE J. Lightw. Technol.*, vol. 31, no. 6, pp. 975–981, Mar. 2013.
[6] P. Dong *et al.*, "Wavelength-tunable silicon microring modulator," *Opt. Express*, vol. 18, no. 11, pp. 10941–10946, May 2010.
[7] Y. Hu *et al.*, "High-speed silicon modulator based on cascaded microring resonators," *Opt. Express*, vol. 20, no. 14, pp. 15079–15085, Jul. 2012.
[8] T. Baba *et al.*, "50-Gb/s ring resonator-based silicon modulator," *Opt. Express*, vol. 21, no. 10, pp. 11869–11876, May 2013.
[9] M. Yang *et al.*, "Non-blocking 4 × 4 electro-optic silicon switch for on-chip photonic networks," *Opt. Express*, vol. 19, no. 1, pp. 47–54, Jan. 2011.
[10] W. Chen *et al.*, "Mach–Zehnder-based four-port switching module on SOI," *IEEE Photon. Technol. Lett.*, vol. 24, no. 15, pp. 1313–1315, Aug. 2012.

[11] W. Chen *et al.*, "A 2 × 2 nonblocking Mach–Zehnder-based silicon switch matrix," *Opt. Express*, vol. 20, no. 11, pp. 12 593–12 598, May 2012.
[12] T. Hu *et al.*, "Wavelength-selective 4 × 4 nonblocking silicon optical router for networks-on-chip," *Opt. Lett.*, vol. 36, no. 23, pp. 4710–4712, 2011.
[13] X. Li *et al.*, "Mach–Zehnder-based five-port silicon router for optical interconnects," *Opt. Lett.*, vol. 38, no. 10, pp. 1703–1705, May 2013.
[14] J. Xing, Z. Li, Y. Yu, and J. Yu, "Low cross-talk 2 × 2 silicon electro-optic switch matrix with a double-gate configuration," *Opt. Lett.*, vol. 38, no. 22, pp. 4774–4776, 2013.
[15] J. V. Campenhout, W. M. J. Green, S. Assefa, and Y. A. Vlasov, "Low-power, 2 × 2 silicon electro-optic switch with 110-nm bandwidth for broadband reconfigurable optical networks," *Opt. Express*, vol. 17, no. 26, pp. 24 020–24 029, Dec. 2009.
[16] G. W. Cong *et al.*, "Large current MOSFET on photonic silicon-on-insulator wafers and its monolithic integration with a thermo-optic 2 × 2 Mach–Zehnder switch," *Opt. Express*, vol. 21, no. 6, pp. 6889–6894, Mar. 2013.
[17] H. Xu *et al.*, "High speed silicon Mach–Zehnder modulator based on interleaved PN junctions," *Opt. Express*, vol. 20, no. 14, pp. 15 093–15 099, Jul. 2012.
[18] J. Song *et al.*, "On-chip quasi-digital optical switch using silicon microring resonator-coupled Mach–Zehnder interferometer," *Opt. Express*, vol. 21, no. 10, pp. 12–767–12–772, May 2013.
[19] P. Dong, S. F. Preble, and M. Lipson, "All-optical compact silicon comb switch," *Opt. Express*, vol. 15, no. 15, pp. 9600–9605, Jul. 2007.